arXiv:1204.1742v1 [quant-ph] 8 Apr 2012

Quantum internet using code division multiple access

Jing Zhang[1,2,3],* Yu-xi Liu[1,3,4], Şahin Kaya Özdemir[1,5], Re-Bing Wu[1,2,3], Xiang-Bin Wang[6], and Franco Nori[1,7]

[1] *Advanced Science Institute, RIKEN, Wako-shi, Saitama 351-0198, Japan*
[2] *Department of Automation, Tsinghua University, Beijing 100084, P. R. China*
[3] *Center for Quantum Information Science and Technology,*
Tsinghua National Laboratory for Information Science and Technology, Beijing 100084, P. R. China
[4] *Institute of Microelectronics, Tsinghua University, Beijing 100084, P. R. China*
[5] *Electrical and Systems Engineering, Washington University, St. Louis, Missouri 63130, USA*
[6] *Department of Physics, Tsinghua University, Beijing 100084, P. R. China*
[7] *Physics Department, The University of Michigan, Ann Arbor, MI 48109-1040, USA*

(Dated: March 2, 2013)

Code division multiple access (CDMA) is a spread-spectrum technology, in which a code is used to spread the spectral content of information to achieve larger network capacity. It has been widely used in classical communication and wireless networks. Here, we extend CDMA to the quantum case, where many pairs of nodes can transmit quantum information through a shared channel. This can be achieved by chaotic encoding of quantum information to spread its spectral content and by chaos synchronization, to separate different sender-receiver pairs. The proposed method is robust to low-frequency noise, and achieves faithful transmission with fidelities of up to 0.99.

PACS numbers: 89.70.-a, 42.79.Sz, 62.25.Jk

Introduction.— Quantum networks (for applications such as long distance communication and distributed computing) require nodes capable of storing and processing quantum information and connected to each other via photonic channels [1]. Recent achievements in quantum computing [2] have brought quantum networking much closer to realization. Quantum networks provide advantages for the transmission of quantum and classical information, after proper encoding into quantum states [3, 4]. However, the efficient transfer of quantum information among many nodes has remained problems yet to be studied [1, 5, 6]. These become crucial for the limited-resource scenarios in large-scale networks. A remedy, inspired from classical communication theory, is to allow simultaneous transmission of multiple quantum data streams to share the same channel or physical medium.

In classical communication networks, multiple-access schemes have been effectively used to allow multi-user access. These multiple-access methods include: either time-division multiple-access (TDMA), frequency-division multiple-access (FDMA), or CDMA, in which each user is assigned a particular time slot, frequency, or code, respectively. In TDMA, the users share the same frequency at different time slots, but timing synchronization and delays become serious problems in large-scale networks. FDMA is bandwidth-limited, which limits the number of users in the network. Unlike TDMA and FDMA, CDMA utilizes the entire spectrum to encode the information from all the users by distinguishing different users with their own unique codes. It is known as spread-spectrum technology. CDMA can accommodate more users per MHz of bandwidth, providing a capacity improvement on the order of 10^4 to 10^6, compared to TDMA and FDMA [8]. Due to these advantages, CDMA achieves great success in commercial applications in classical communication (e.g., more than 50% of the mobile phones currently use the CDMA technique).

These multiple-access techniques should be applicable to quantum networks using either classical or quantum multiplexers. FDMA has already been used in quantum key distribution (QKD) networks [7] using conventional classical wavelength division multiplexers. An alternative approach would be to introduce quantum multiplexers which transform the input quantum states from different users into a quantum superposition state and then send it through a single channel [see Fig. 1(a)]. Such quantum multiplexers have not been demonstrated yet. Moreover, despite its success in classical networks, to the best of our knowledge, CDMA has not been used in quantum networks and internet [1]. The use of CDMA in quantum networks holds the potential to provide advantages for multi-channel quantum information transmission, like in classical communication networks.

In this work, we extend the concept of CDMA to its quantum version. This extension is not straightforward, because in the quantum case, the information transmitted in the channel is formed by the superposition of quantum states sent by different nodes. This makes it difficult to coherently and faithfully extract information for each receiver node. Moreover, the quantum state transmitted through the channel is prone to noises, whose deteriorating effects should be minimized.

We show that obstacles towards quantum CDMA (Q-CDMA) can be overcome via chaotic encoding and chaos synchronization among senders and receivers, which also suppresses low-frequency noises. To achieve this, it is necessary to have a quantum channel to transmit quantum superposition state and N classical channels to achieve chaotic synchronization to decode the quantum signals at the receivers.

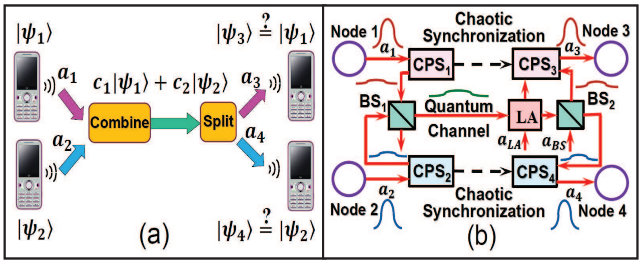

FIG. 1: (color online) (a) Quantum information transmission between two pairs of nodes via a single quantum channel. Quantum states from two senders are combined to form a superposition state and input to the channel. At the receiver side, they are coherently split into two and sent to the targeted receivers. (b) Schematic diagram of the quantum code-division multiple-access (Q-CDMA) network by chaotic synchronization. Wave packets from the sender nodes are first spectrally broadened by using the chaotic phase shifters CPS_1 and CPS_2, and then mixed at a beamsplitter (BS_1) and input to the channel. Individual signals are recovered at the receiver end with the help of CPS_3 and CPS_4, which are synchronized with CPS_1 and CPS_2, respectively.

Quantum CDMA network.— To present the underlying principle of our scheme, we consider the simplest case, where two pairs of sender and receiver nodes communicate quantum information via a single quantum channel [see Fig. 1(a)]. The quantum information from different users is encoded into quantized electromagnetic fields having the *same* frequencies.

The schematic diagram of our strategy is shown in Fig. 1(b). The quantum information sent by the nodes 1 and 2 is first encoded by two chaotic phase shifters CPS_1 and CPS_2, whose operation can be modelled by the effective Hamiltonian $\delta_i(t)\, a_i^\dagger a_i$, with $\delta_i(t)$ being time-dependent classical chaotic signals and $i = 1, 2$. Hereafter, we set $\hbar = 1$. The two beams are combined by a $50:50$ beamsplitter BS_1 and then transmitted via a quantum channel. At the end of the quantum channel, the quantum signal is amplified by a phase-insensitive linear amplifier (LA) and then divided into two branches by a second 50:50 beamsplitter BS_2 and sent to nodes 3 and 4 through two chaotic phase shifters CPS_3 and CPS_4. CPS_3 and CPS_4 are introduced to decode the information by applying the effective Hamiltonian $-\delta_j(t)\, a_j^\dagger a_j$, with $j = 3, 4$. Amplifier gain is set to $G = 4$, to compensate the losses induced by the beamsplitters. Quantum interference of signals from different chaotic sources has recently been demonstrated [10], suggesting the feasibility of the scheme proposed here.

The actions of the chaotic devices $\text{CPS}_{i=1,2,3,4}$ induce the phase shifts $\exp\left[-i\theta_i(t)\right]$, where $\theta_i(t) = \int_0^t \delta_i(\tau)\, d\tau$. Thus, to achieve faithful transmission between the senders and the receivers, the effects of $\delta_1(t)$ and $\delta_2(t)$ on the quantum signals should be minimized in the fields received by the nodes 3 and 4. Intuitively, this could be done by simply adjusting the system parameters such that $\delta_1(t) = \delta_3(t)$ and $\delta_2(t) = \delta_4(t)$. However, such an approach is impractical, because any small deviation in the system parameters can be greatly amplified by the chaotic motion, making it impossible to keep two chaotic circuits with the same exact parameters and initial conditions. Instead, auxiliary classical channels between senders and the intended receivers can be used to synchronize the chaotic circuit as shown in Fig. 1(b). This classical chaotic synchronization enables to reduce the parameter differences between the chaotic phase shifters and to extract the quantum information faithfully.

Hereafter, for the sake of simplicity, we assume that CPS_1 (CPS_2) and CPS_3 (CPS_4) have been synchronized before the start of the transmission of quantum information, i.e., $\theta_1(t) = \theta_3(t)$ [$\theta_2(t) = \theta_4(t)$]. The whole information transmission process can be described by the input-output relationship of the quantum network (see Eq. (8) in Ref. [12])

$$\begin{aligned} a_3 &= a_1 + a_2 e^{i(\theta_1-\theta_2)} + \frac{\sqrt{6}}{2} e^{i\theta_1} a_{\text{LA}}^\dagger + \frac{1}{\sqrt{2}} e^{i\theta_1} a_{\text{BS}}, \\ a_4 &= a_2 + a_1 e^{i(\theta_2-\theta_1)} + \frac{\sqrt{6}}{2} e^{i\theta_2} a_{\text{LA}}^\dagger - \frac{1}{\sqrt{2}} e^{i\theta_2} a_{\text{BS}}, \end{aligned} \tag{1}$$

where $a_{\text{LA}}^\dagger$ and a_{BS} are the creation and annihilation operators of the auxiliary vacuum fields entering the linear amplifier LA and the second beamsplitter BS_2. For the pseudo-noise chaotic phase-shift $\theta_i(t)$, we should take an average over this broadband random signal [11], which leads to $\overline{\exp\left(\pm i\theta_i(t)\right)} \approx \sqrt{M_i}$ (see Eq. (3) in [12]) with

$$M_i = \exp\left[-\pi \int_{\omega_{li}}^{\omega_{ui}} d\omega\; S_{\delta_i}(\omega) / \omega^2\right]. \tag{2}$$

In Eq. (2), $S_{\delta_i}(\omega)$ is the power spectrum density of the signal $\delta_i(t)$, and ω_{li} and ω_{ui} are the lower and upper bounds of the frequency band of $\delta_i(t)$, respectively. Equation (1) can then be reduced to

$$\begin{aligned} a_3 &= a_1 + \sqrt{M_1 M_2}\, a_2 + \sqrt{\frac{3M_1}{2}} a_{\text{LA}}^\dagger + \sqrt{\frac{M_1}{2}} a_{\text{BS}}, \\ a_4 &= a_2 + \sqrt{M_1 M_2}\, a_1 + \sqrt{\frac{3M_1}{2}} a_{\text{LA}}^\dagger - \sqrt{\frac{M_2}{2}} a_{\text{BS}}. \end{aligned} \tag{3}$$

For a chaotic signal with broadband frequency spectrum, the factor M_i is extremely small, and can be neglected in Eq. (3). This leads to $a_3 \approx a_1$ and $a_4 \approx a_2$, implying efficient and faithful transmission of quantum information from nodes 1 and 2 to nodes 3 and 4, respectively.

The information-bearing fields a_1 and a_2, having the same frequency ω_c, are modulated by two different pseudo-noise signals, which not only broaden them in the frequency domain but also change the shape of their wavepackets [see Fig. 1(b)]. Thus, the energies of the fields a_1 and a_2 are distributed within a very broad frequency span, in which the contribution of ω_c is extremely small and impossible to extract without coherent sharpening of the ω_c components. This, on the other hand, is possible only via chaotic synchronization which effectively eliminates the effect of the pseudo-noises on the fields and enables the recovery of a_1 (a_2) at the output a_3 (a_4) with almost no disturbance from a_2 (a_1). This is similar to the CDMA in classical communication. Thus, we name our scheme as Q-CDMA network.

Quantum state transmission.— Let us further study the transmission of qubit states over the proposed Q-CDMA network using a concrete model. The qubit states $\{|\phi_1\rangle = \sqrt{p_1}|g_1\rangle + \sqrt{1-p_1}|e_1\rangle$, and $|\phi_2\rangle = \sqrt{p_2}|g_2\rangle + \sqrt{1-p_2}|e_2\rangle$, with $p_1, p_2 \in [0,1]\}$, to be transmitted are encoded in the dark states of two Λ-type three-level atoms; i.e., atom 1 in cavity 1 and atom 2, in cavity 2, as shown in Fig. 2. The qubit states are transferred to the cavities by Raman transitions and are transmitted over the Q-CDMA network. At the receiver nodes, the quantum states are transferred and stored in two Λ-type atoms; i.e., atom 3 in cavity 3, and atom 4 in cavity 4. We assume that the four coupled atom-cavity systems have the same parameters. Let $|g_i\rangle$, $|e_i\rangle$, and $|r_i\rangle$ be the three energy levels of atom i. As shown in Fig. 2, the $|g_i\rangle \to |r_i\rangle$ and $|e_i\rangle \to |r_i\rangle$ transitions are coupled with a classical control field and a quantized cavity field with coupling strengths $\Omega_i(t)$ and g. By adiabatically eliminating the highest energy level $|r_i\rangle$, the Hamiltonian of the atom-cavity system can be expressed as

$$H_i = g_i(t)\left(c_i|e_i\rangle\langle g_i| + c_i^\dagger|g_i\rangle\langle e_i|\right), \tag{4}$$

where c_i is the annihilation operator of the i-th cavity mode; $g_i(t) = g\Omega_i(t)/\Delta$ is the coupling strength which can be tuned by the classical control field $\Omega_i(t)$; and Δ is the atom-cavity detuning. The cavity fields c_i are related to the travelling fields a_i by

$$\begin{aligned} a_1 &= \sqrt{\kappa}\, c_1 + a_{1,\text{in}}, \quad & a_2 &= \sqrt{\kappa}\, c_2 + a_{2,\text{in}}, \\ a_{3,\text{out}} &= \sqrt{\kappa}\, c_3 + a_3, \quad & a_{4,\text{out}} &= \sqrt{\kappa}\, c_4 + a_4, \end{aligned} \tag{5}$$

where κ is the decay rate of the cavity field; and $a_{1,\text{in}}$, $a_{2,\text{in}}$ (both in vacuum states) and $a_{3,\text{out}}$, $a_{4,\text{out}}$ are the input and output fields of the whole system, respectively.

The chaotic phase shifters $\text{CPS}_{i=1,2,3,4}$ are realized by coupling the optical fields to four driven Duffing oscillators, with damping rates γ, described by the Hamiltonian

$$H_{\text{Duff},i} = \frac{\omega_o}{2}p_i^2 + \frac{\omega_o}{2}x_i^2 - \mu x_i^4 - f(t)\,x_i, \tag{6}$$

where x_i and p_i are the normalized position and momentum of the nonlinear Duffing oscillators, $\omega_0/2\pi$ is the frequency of the fundamental mode, μ is a nonlinear constant, and $f(t) = f_d\cos(\omega_d t)$ is the driving force.

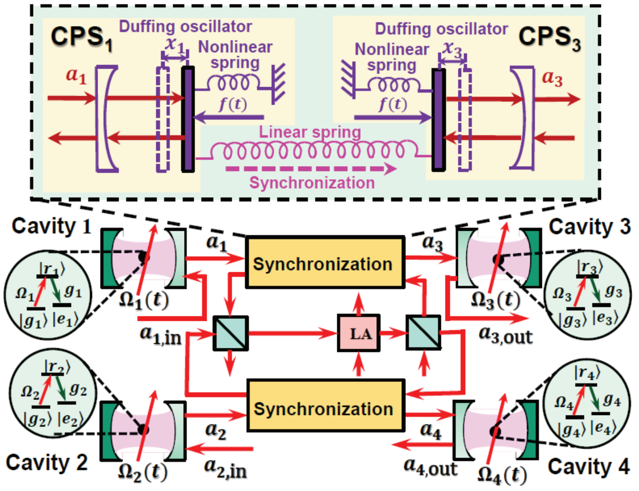

FIG. 2: (color online) Schematic diagram of quantum state transmission over quantum CDMA network.

The interaction between the field a_i and the i-th Duffing oscillator is given by the Hamiltonian $H_i = g_{\text{f-o}}x_i a_i^\dagger a_i$, where $g_{\text{f-o}}$ is the coupling strength between the field and the oscillator. In optomechanical systems, such an interaction Hamiltonian can be realized by coupling the optical field via the radiation pressure to a moving mirror connected to a nonlinear spring (see Fig. 2). Under the semiclassical approximation for the degrees of freedom of the oscillator, the interaction Hamiltonian H_i leads to a phase factor $\exp\left[-i\int_0^t g_{\text{f-o}}x_i(\tau)\,d\tau\right]$ for the field a_i. To simplify the discussion, we assume that all of the four Duffing oscillators have the same ω_0, μ, f_d, and ω_d, but different initial states. Finally, the chaotic synchronization between CPS_1 (CPS_2) and CPS_3 (CPS_4) is achieved by coupling two Duffing oscillators by a harmonic potential $V(x_1, x_3) = k_I(x_1 - x_3)^2/2$, which can be realized, e.g., in mechanical systems, by coupling the two oscillators via a linear spring with stiffness k_I. Such kind of synchronization of mechanical oscillators have been realized in experiments (see, e.g., Ref. [13]).

To show the efficiency of state transmission in Q-CDMA, let us calculate the fidelities $F_1 = \langle\phi_1|\rho_3|\phi_1\rangle$ and $F_2 = \langle\phi_2|\rho_3|\phi_2\rangle$, where ρ_3 and ρ_4 are the quantum states received by atom 3 and atom 4, and $|\phi_1\rangle = \sqrt{p_0}|g_1\rangle + \sqrt{1-p_0}|e_1\rangle$ and $|\phi_2\rangle = \sqrt{1-p_0}|g_2\rangle + \sqrt{p_0}|e_2\rangle$ are the two quantum states to be transmitted. By designing the control parameters $g_i(t)$, using the method given in Ref. [5], we find that the fidelities F_1 and F_2 are independent of the transmitted quantum states parameterized by p_0 and just depend on the correction factor $M = M_1 = M_2 \ll 1$ which can be approximated as $F_1 = F_2 \approx 1 - M$, by neglecting the M^2 terms (see Eq. (33) in [12]). When the Duffing oscillator enters the chaotic regime, we have $M \approx 0$, leading to fidelities F_1, $F_2 \approx 1$, which means that the qubit states can be faithfully transmitted over the Q-CDMA network.

Numerical simulations.— Here we show the feasibility of the Q-CDMA scheme using numerical simulations with the system parameters $\omega_d/\omega_0 = 5$, $g_{\text{f-o}}/\omega_0 = 0.03$, $\mu/\omega_0 = 0.25$, $\gamma/\omega_0 = 0.05$, $k_I/\omega_0 = 0.1$, and $p_0 = 0.6$. In Fig. 3(a), it is seen that there are three distinct regions representing how the chaotic motion affects the fidelity of the quantum state transmission. In the periodic regime ($0 < f_d/\omega_0 < 15$), both F_1 and F_2 experience slight increases with increasing f_d/ω_0, with $0.4 < F_1 < 0.5$ and $0.6 \leq F_2 \leq 0.64$. At $f_d/\omega_0 = 15$, the soft-chaotic regime of the Duffing oscillator start, indicated by a positive Lyapunov exponential $\lambda \approx 0.038$ and a sudden jump in fidelities. In this regime, delineated by $15 \leq f_d/\omega_0 \leq 33$, both F_1 and F_2 are still below 0.7. The dynamics of the Duffing oscillator enters the hard-chaos regime at $f_d/\omega_0 \approx 33$, where both F_1 and F_2 jumps suddenly to 1, which corresponds to an almost 100% faithful state transmission.

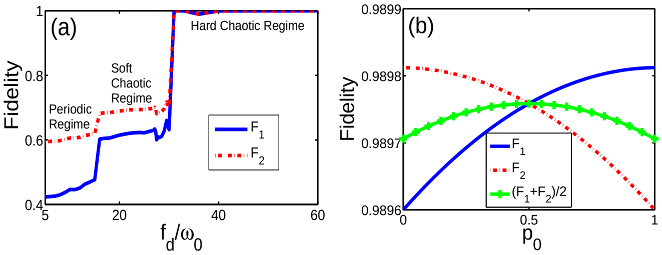

FIG. 3: (color online) (a) Fidelities F_1 and F_2 versus the strength f_d of the driving force acting on the Duffing oscillator with $p_0 = 0.6$, and $\tau = 2\pi/\omega_0$ as the unit of time. (b) F_1, F_2 and their average $(F_1 + F_2)/2$ versus p_0 in the hard-chaotic region, with $f_d/\omega_0 = 36$. The average fidelity is maximized at $p_0 = 0.5$, which corresponds to $|\phi_1\rangle = |\phi_2\rangle$.

In Fig. 3(b), we plot the trajectories of F_1 and F_2 as a function of p_0 in the hard-chaotic regime $f_d/\omega_0 = 36$, corresponding to $M \approx 0.0103$. It is seen that F_1 and F_2 are very close to $1 - M \approx 0.9897$ and almost constant regardless of the value of p_0. There are small deviations from $1 - M$, because here M^2 terms are not neglected. The average fidelity $\bar{F} = (F_1 + F_2)/2$ is maximum at $p_0 = 1/2$, which corresponds to an equally-weighted superposition of the quantum states $|\phi_1\rangle$ and $|\phi_2\rangle$. In such a case, the crosstalk between the channels becomes minimum, inducing only a very slight disturbance on these indistinguishable states.

Robustness to low-frequency noise.— Our scheme is robust to low-frequency noises in the quantum channel between BS_1 and the LA of Fig. 2. To show this, we express the quantum field transmitted in the channel by the annihilation operator $\tilde{c} = c + n$, where $c = e^{i\theta_1}a_1/\sqrt{2} + e^{i\theta_2}a_2/\sqrt{2}$ is the annihilation operator of the information bearing field, $n = \sum_{\omega\in[\omega_{l0},\omega_{u0}]}\left(A_\omega e^{-i\omega t} + \text{h.c.}\right)$ is the noise term, A_ω denotes the amplitude of the noise component with frequency ω, and ω_{l0}, ω_{u0} are the lower and upper bounds of the frequency band of the noise n, respectively. Then the fields entering the cavities 3 and 4 of Fig. 2 are expressed as $\tilde{a}_i = a_i + n\exp\left[i\theta_i\left(t\right)\right]$, with a_i given in Eq. (3) and $i = 3, 4$. Since the noise n is mainly distributed in the low-frequency regime, the phase shift $\theta_i\left(t\right)$ can be divided into a low-frequency part $\theta_{li}\left(t\right)$ and a high-frequency part $\theta_{hi}\left(t\right)$, where $\theta_{hi}\left(t\right)$ is the combination of those components much faster than those of $n\left(t\right)$, i.e., the components with frequencies $\omega \in [\tilde{\omega}_{li}, \omega_{ui}]$ and $\tilde{\omega}_{li} \gg \omega_{u0}$. By averaging over the high-frequency components, we have $\tilde{a}_i = a_i + \sqrt{\tilde{M}_i}ne^{\theta_{li}(t)}$, where $\tilde{M}_i = \exp\left[-\pi\int_{\tilde{\omega}_{li}}^{\omega_{ui}} d\omega S_{\delta_i}(\omega)/\omega^2\right]$. Since $\tilde{M}_i$ is still very small, we have $\tilde{a}_i \approx a_i$, which means that the noise effects are significantly reduced by chaotic synchronization. Additional calculations show that the noise n leads to high-order correction terms like $\tilde{M}_1 M$ and $\tilde{M}_2 M$ which can be neglected, without affecting F_1 and F_2. Thus, we conclude that our scheme is robust against low-frequency noises in the quantum channel.

Conclusions.— We have introduced a Q-CDMA network based on chaotic synchronization where quantum information can be faithfully transmitted with fidelities as high as 0.99 between multiple pairs of nodes sharing a single quantum channel. The proposed quantum multiple-access network is robust against low-frequency noises. Chaotic phase shifters and their synchronization required for the proposed Q-CDMA can be implemented in various systems, such as optomechanical and solid-state quantum systems. In particular, whispering-gallery-mode optical resonators (e.g., microtoroid, microdisk, microring, etc) are ideal platforms. Chaotic behavior in an optical-fiber-coupled microtoroid resonator has been reported in Ref. [14], and the synchronization of mechanical modes in two spatially-separated microring resonators coupled via waveguides has been proposed in Ref. [15], suggesting that our proposal is not far from practical realization. Owing to the rapid pace of experimental and theoretical developments, we believe that our proposal will soon be able to pave the way for long distance Q-CDMA networks, and will give new perspectives for the optimization of quantum networks.

JZ thanks Dr. X.Y.Lü for helpful discussions. FN acknowledges partial support from the NSA, LPS, ARO, NSF grant No. EIA-0130383, and from JSPS-RFBR 06-02-91200. JZ and RBW are supported by the NSFC under Grant Nos. 61174084, 61134008, 60904034. YXL is supported by the NSFC under Grant Nos. 10975080, 61025022, 60836001. ŞKÖ thanks Dr. L. Yang for support.

---

[*] Electronic address: jing-zhang@mail.tsinghua.edu.cn

[1] H. J. Kimble, Nature **453**, 1023 (2008); D. Felinto, C. W. Chou, J. Laurat, E. W. Schomburg, H. de Riedmatte, and

H. J. Kimble, Nature Phys. **2**, 844 (2006); C.-W. Chou, J. Laurat, H. Deng, K. S. Choi, H. de Riedmatten, D. Felinto, and H. J. Kimble, Science **316**, 1316 (2007).

[2] M. D. Lukin, Rev. Mod. Phys. **75**, 457 (2003); N. Sangouard, C. Simon, H. de Riedmatten, and N. Gisin, Rev. Mod. Phys. **83**, 33 (2011); J. Q. You and F. Nori, Physics Today **58** (11), 42 (2005); Nature **474**, 589 (2011); J. Clarke and F. K. Wilhelm, Nature **453**, 1031 (2008); I. Buluta, S. Ashhab, and F. Nori, Rep. Prog. Phys. **74**, 104401 (2011); R. Blatt and D. J. Wineland, Nature **453**, 1008 (2008).

[3] G. Smith and J. Yard, Science **321**, 1812 (2008); L. Czekaj and P. Horodecki, Phys. Rev. Lett. **102**, 110505 (2009); M. Heurs, J. G. Webb, A. E. Dunlop, C. C. Harb, T. C. Ralph, and E. H. Huntington, Phys. Rev. A **81**, 032325 (2010).

[4] N. Gisin, G. Ribordy, W. Tittel, and H. Zbinden, Rev. Mod. Phys. **74**, 145 (2002); X. B. Wang, T. Hiroshima, A. Tomita, and M. Hayashi, Phys. Rep. **448**, 1 (2007); J.-W. Pan, Z.-B. Chen, C.-Y. Lu, H. Weinfurter, A. Zeilinger, M. Zukowski, arXiv:0805.2853v2.

[5] J. I. Cirac, P. Zoller, H. J. Kimble, and H. Mabuchi, Phys. Rev. Lett. **78**, 3221 (1997); S. J. Van Enk, J. I. Cirac, P. Zoller, H. J. Kimble, and H. Mabuchi, J. Mod. Opt. **44**, 1727 (1997).

[6] X. Maitre, E. Hagley, G. Nogues, C. Wunderlich, P. Goy, M. Brune, J. M. Raimond, and S. Haroche, Phys. Rev. Lett. **79**, 769 (1997); D. F. Phillips, A. Fleischhauer, A. Mair, and R. L. Walsworth, and M. D. Lukin, Phys. Rev. Lett. **86**, 783 (2001); L. M. Duan, M. D. Lukin, J. I. Cirac, and P. Zoller, Nature **414**, 413 (2001); D. N. Matsukevich and A. Kuzmich, Science **306**, 663 (2004); A. Acín, J. I. Cirac, and M. Lewenstein, Nature Phys. **3**, 256 (2007); X. Y. Lü, J. B. Liu, C. L. Ding, and J. H. Li Phys. Rev. A **78**, 032305 (2008).

[7] K. Yoshino, M. Fujiwara, A. Tanaka, S. Takahashi, Y. Nambu, A. Tomita, S. Miki, T. Yamashita, Z. Wang, M. Sasaki, and A. Tajima, Opt. Lett. **37**, 223 (2012); G. Brassard, F. Bussieres, N. Godbout, and S. Lacroix, AIP Conf. Proc. **734**, 323 (2004); A. Ortigosa-Blanch and J. Capmany, Phys. Rev. A **73**, 024305 (2006); G. Brassard, F. Bussieres, N. Godbout, and S. Lacroix, Proc. SPIE **5260**, 149 (2003); P. Townsend, Electron. Lett. **33**, 188 (1997).

[8] K. S. Gilhousen, I. M. Jacobs, R. Padovani, A. J. Viterbi, L. A. Weaver, and C. E. Wheatley, IEEE Trans. Veh. Technol. **40**, 303 (1991).

[9] R. Rom and M. Sidi, *Multiple Access Protocols: Performance and Analysis* (Springer-Verlag, New York, 1990); V. P. Ipatov, *Spread Spectrum and CDMA: Principles and Applications* (Wiley, England, 2005).

[10] A. Nevet, A. Hayat, P. Ginzburg, and M. Orenstein, Phys. Rev. Lett. **107**, 253601 (2011).

[11] J. Zhang, Y. X. Liu, W. M. Zhang, L. A. Wu, R. B. Wu, and T. J. Tarn, Phys. Rev. B **84**, 214304 (2011).

[12] See the supplementary information.

[13] S.-B. Shim, M. Imboden, and P. Mohanty, Science **316**, 95 (2007).

[14] T. Carmon, M. C. Cross, and K. J. Vahala, Phys. Rev. Lett. **98**, 167203 (2007).

[15] S. Manipatruni, G. Wiederhecker, and M. Lipson, Quantum Electronics and Laser Science Conference, Baltimore, Maryland, May 2011.

arXiv:1204.1742v1 [quant-ph] 8 Apr 2012

Supplement to "Quantum internet using code division multiple access"

Jing Zhang[1,2,3],* Yu-xi Liu[1,3,4], Şahin Kaya Özdemir[1,5], Re-Bing Wu[1,2,3], Xiang-Bin Wang[6], and Franco Nori[1,7]

[1] *Advanced Science Institute, RIKEN, Wako-shi, Saitama 351-0198, Japan*
[2] *Department of Automation, Tsinghua University, Beijing 100084, P. R. China*
[3] *Center for Quantum Information Science and Technology,*
Tsinghua National Laboratory for Information Science and Technology, Beijing 100084, P. R. China
[4] *Institute of Microelectronics, Tsinghua University, Beijing 100084, P. R. China*
[5] *Electrical and Systems Engineering, Washington University, St. Louis, Missouri 63130, USA*
[6] *Department of Physics, Tsinghua University, Beijing 100084, P. R. China*
[7] *Physics Department, The University of Michigan, Ann Arbor, MI 48109-1040, USA*

(Dated: March 2, 2013)

PACS numbers: 89.70.-a, 42.79.Sz, 62.25.Jk

This supplementary material presents derivations on the following topics: (1) how to average out the chaotic phase shift; (2) derivations of the input-output relationship of the quantum CDMA network; (3) derivations about the quantum state transmission over the quantum CDMA network; and (4) analysis of the chaotic synchronization of the Duffing oscillators.

AVERAGING OVER THE CHAOTIC PHASE SHIFT

Since the chaotic signal $\delta_i(t)$ can be expressed as a combination of many high-frequency components, i.e.,

$$\delta_i(t) = \sum_\alpha A_{i\alpha} \cos\left(\omega_{i\alpha} t + \phi_{i\alpha}\right), \tag{1}$$

where $A_{i\alpha}$, $\omega_{i\alpha}$, $\phi_{i\alpha}$ are the amplitude, frequency, and phase of each component, we can obtain

$$\theta_i(t) = \int_0^t \delta_i(\tau)\, d\tau = \sum_\alpha \frac{A_{i\alpha}}{\omega_{i\alpha}} \sin\left(\omega_{i\alpha} t + \phi_{i\alpha}\right).$$

Using the Fourier-Bessel series identity [1, 2]: $\exp\left(ix \sin y\right) = \sum_n J_n(x) \exp\left(iny\right)$, with $J_n(x)$ as the n-th Bessel function of the first kind, it can be calculated

$$\exp\left[-i\theta_i(t)\right] = \prod_\alpha \left[\sum_{n_\alpha} J_{n_\alpha}\!\left(\frac{A_{i\alpha}}{\omega_{i\alpha}}\right) e^{-in_\alpha \omega_{i\alpha} t - in_\alpha \phi_{i\alpha}}\right].$$

Let us take average over the "random" phase $\theta_i\left(t\right)$ [3], the components related to the frequencies $\omega_{i\alpha}$ should be looked as fast-oscillating terms and thus can be averaged out. The above treatment corresponds to averaging out the components that are far off resonance with the information-bearing field, and keep the near-resonance components. Only the lowest-frequency terms, with $n_\alpha = 0$, dominate the dynamical evolution. Thus, we have

$$\overline{\exp\left[-i\theta_i(t)\right]} = \prod_\alpha \left[J_0\!\left(\frac{A_{i\alpha}}{\omega_{i\alpha}}\right)\right]. \tag{2}$$

Since the chaotic signal $\delta_i(t)$ is mainly distributed in the high-frequency regime, we have $A_{i\alpha} \ll \omega_{i\alpha}$. Thus, from the approximation $J_0(x) \approx 1 - x^2/4$, $\log\left(1+x\right) \approx x$ for $x \ll 1$, it can be calculated that

$$\begin{aligned}\prod_\alpha J_0\!\left(\frac{A_{i\alpha}}{\omega_{i\alpha}}\right) &= \exp\left[\sum_\alpha \log J_0\!\left(\frac{A_{i\alpha}}{\omega_{i\alpha}}\right)\right] \\ &= \exp\left(-\frac{1}{4}\sum_\alpha \frac{A_{i\alpha}^2}{\omega_{i\alpha}^2}\right) \\ &= \exp\left(-\frac{\pi}{2}\int_{\omega_{li}}^{\omega_{ui}} \frac{S_{\delta_i}\left(\omega\right)}{\omega^2} d\omega\right) \\ &= \sqrt{M_i},\end{aligned} \tag{3}$$

where

$$M_i = \exp\left(-\pi \int_{\omega_{li}}^{\omega_{ui}} \frac{S_{\delta_i}\left(\omega\right)}{\omega^2} d\omega\right).$$

From Eqs. (2) and (3), we can obtained the equation

$$\overline{\exp\left[-i\theta_i\left(t\right)\right]} = \sqrt{M_i}. \tag{4}$$

INPUT-OUTPUT RELATIONSHIP OF THE QUANTUM CDMA NETWORK

Let us calculate the input-output relationship of the quantum CDMA network shown in Fig. 1

As shown in Fig. 1, the input-output relationships of the chaotic phase shifters $\mathrm{CPS}_{i=1,2,3,4}$ can be expressed as

$$\begin{aligned} a_1' = a_1 e^{-i\theta_1}, \quad a_2' = a_2 e^{-i\theta_2}, \\ a_3 = a_3' e^{i\theta_1}, \quad a_4 = a_4' e^{i\theta_2}, \end{aligned} \tag{5}$$

and the input-output relationships of the two beam splitters BS_1 and BS_2 and the linear quantum amplifier "LA" can be expressed as
BS_1:

$$a_5 = \frac{1}{\sqrt{2}} a_1' + \frac{1}{\sqrt{2}} a_2', \quad a_6 = \frac{1}{\sqrt{2}} a_1' - \frac{1}{\sqrt{2}} a_2', \tag{6}$$

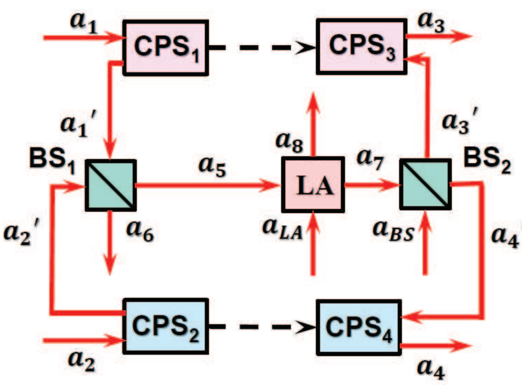

FIG. 1: (color online) Schematic diagram of the quantum CDMA network considered here. The black dashed lines denote the desired chaotic synchronization channel. The red lines show the quantum optical channels. "LA" refers to linear amplifier. "BS" refers to beamsplitter. "CPS" denotes chaotic phase shifter.

LA:

$$a_7 = 2a_5 + \sqrt{3}a_{\rm LA}^{\dagger}, \quad a_8 = \sqrt{3}a_5^{\dagger} + 2a_{\rm LA}, \tag{7}$$

BS$_2$:

$$a_3' = \frac{1}{\sqrt{2}}a_7 + \frac{1}{\sqrt{2}}a_{\rm BS}, \quad a_4' = \frac{1}{\sqrt{2}}a_7 - \frac{1}{\sqrt{2}}a_{\rm BS}. \tag{8}$$

From Eqs. (5-8), we can obtain the total input-output relationship of the quantum network

$$\begin{aligned} a_3 &= a_1 + a_2 e^{i(\theta_1-\theta_2)} + \frac{\sqrt{6}}{2}e^{i\theta_1}a_{\rm LA}^{\dagger} + \frac{1}{\sqrt{2}}e^{i\theta_1}a_{\rm BS}, \\ a_4 &= a_2 + a_1 e^{i(\theta_2-\theta_1)} + \frac{\sqrt{6}}{2}e^{i\theta_2}a_{\rm LA}^{\dagger} - \frac{1}{\sqrt{2}}e^{i\theta_2}a_{\rm BS}. \end{aligned} \tag{9}$$

Here θ_1 and θ_2 come from unsynchronized chaotic signals and thus can be looked as independent "noises".

QUANTUM STATE TRANSMISSION OVER THE QUANTUM CDMA NETWORK

Let us now derive the dynamical equation of the quantum CDMA network used to transmit quantum states. Here, we use the Cirac-Zoller-Kimble-Mabuchi strategy given in Ref. [4] to transmit quantum states. The quantum states $|\phi_1\rangle = \sqrt{r_0}|g_1\rangle + \sqrt{1-r_0}|e_1\rangle$ and $|\phi_2\rangle = \sqrt{1-r_0}|g_2\rangle + \sqrt{r_0}|e_2\rangle$ are encoded in the dark states of two Λ-shaped three-level atoms in cavity 1 and cavity 2. We want to send them to the other two Λ-shaped three-level atoms in the cavity 3 and cavity 4 (see Fig. 2). Let $|g_i\rangle$, $|e_i\rangle$, $|r_i\rangle$ be the three energy levels of the i-th atom. The $|g_i\rangle \to |r_i\rangle$ transition of the atom i is coupled with a classical control field with coupling strength $\Omega_i(t)$ and the $|e_i\rangle \to |r_i\rangle$ transition is coupled with the cavity mode with frequency ω_d and coupling strength g. By adiabatically eliminating the energy level $|r_i\rangle$ (see, e.g., Ref. [5]), we can obtain the following simplified Hamiltonian of the i-th coupled atom-cavity system

$$H_i = g_i(t)\left(c_i|e_i\rangle\langle g_i| + c_i^{\dagger}|g_i\rangle\langle e_i|\right), \tag{10}$$

where c_i is the annihilation operator of the i-th cavity mode; $g_i(t) = g\Omega_i(t)/(2\Delta)$ is the reduced coupling strength between $|g_i\rangle$ and $|e_i\rangle$; $\Delta = \omega_d - \omega_0$ is the detuning of the frequency between the cavity mode and the atom; and $\omega_0 = E_r - E_g = E_r - E_e$ is the energy difference between the ground states $|e_i\rangle$ ($|g_i\rangle$) and excited state $|r_i\rangle$ of the three-level atom. Here, to simplify our discussions, we have omitted the frequency-shift terms induced by the atom-cavity interaction, which can be easily compensated by tuning the frequency ω_d and introducing an additional controllable phase-shift term by the classical control field acting on the i-th atom (see Ref. [4]).

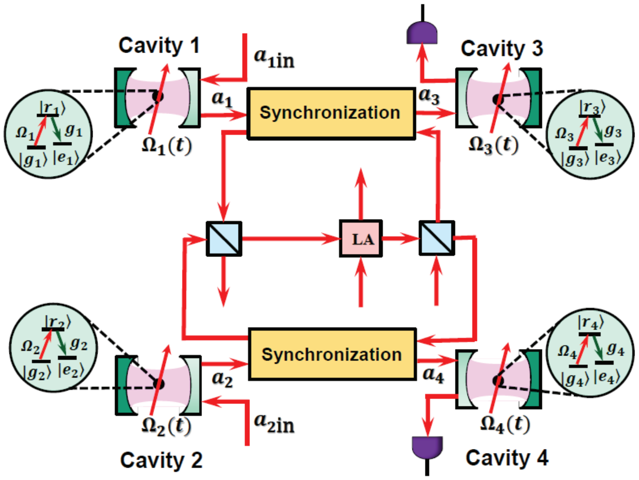

FIG. 2: (color online) Schematic diagram of quantum state transmission over a quantum CDMA network. The broom-shaped or shovel-shaped purple symbols denote photon detectors. The red arrow inside each (green) cavity denotes the classical driving field with amplitude $\Omega_i(t)$ $(i = 1, 2, 3, 4)$. The green circles denote Λ-type three-level atoms.

The complete Hamiltonian of the whole system shown in Fig. 2 is

$$\begin{aligned} H &= \sum_{i=1}^{4} H_i + i\sqrt{\kappa}\left(c_3 a_3^{\dagger} - c_3^{\dagger}a_3\right) + i\sqrt{\kappa}\left(c_4 a_4^{\dagger} - c_4^{\dagger}a_4\right) \\ &\quad + i\sqrt{\kappa}\left(c_1 a_{1,\rm in} - c_1^{\dagger}a_{1,\rm in}\right) + i\sqrt{\kappa}\left(c_2 a_{2,\rm in}^{\dagger} - c_2^{\dagger}a_{2,\rm in}\right), \end{aligned} \tag{11}$$

where κ is the decay rate of the cavity mode introduced by the external input fields $a_{1,\rm in}$, $a_{2,\rm in}$, a_3, and a_4. From the input-output theory, the output fields a_1 and a_2 of the cavity 1 and cavity 2 can be expressed as

$$a_1 = \sqrt{\kappa} c_1 + a_{1,\mathrm{in}}, \quad a_2 = \sqrt{\kappa} c_2 + a_{2,\mathrm{in}}. \qquad (12)$$

Recall that the input-output relationship of the quantum CDMA network can be written as

$$\begin{aligned} a_3 &= a_1 + M a_2 + \frac{\sqrt{6M}}{2} a_{\mathrm{LA}}^{\dagger} + \sqrt{\frac{M}{2}} a_{\mathrm{BS}}, \\ a_4 &= a_2 + M a_1 + \frac{\sqrt{6M}}{2} a_{\mathrm{LA}}^{\dagger} - \sqrt{\frac{M}{2}} a_{\mathrm{BS}}. \qquad (13) \end{aligned}$$

Substituting Eqs. (12) and (13) into Eq. (11), the total Hamiltonian can be re-expressed as

$$\begin{aligned} H &= \sum_{i=1}^{4} H_i + i\kappa \left[c_3 \left(c_1^{\dagger} + M c_2^{\dagger} \right) - c_3^{\dagger} \left(c_1 + M c_2 \right) \right] \\ &\quad + i\kappa \left[c_4 \left(c_2^{\dagger} + M c_1^{\dagger} \right) - c_4^{\dagger} \left(c_2 + M c_1 \right) \right] \\ &\quad + i\sqrt{\kappa} \left[\left(c_1 + c_3 + M c_4 \right) a_{1,\mathrm{in}}^{\dagger} \right. \\ &\quad \left. - \left(c_1^{\dagger} + c_3^{\dagger} + M c_4^{\dagger} \right) a_{1,\mathrm{in}} \right] \\ &\quad + i\sqrt{\kappa} \left[\left(c_2 + c_4 + M c_3 \right) a_{2,\mathrm{in}}^{\dagger} \right. \\ &\quad \left. - \left(c_2^{\dagger} + c_4^{\dagger} + M c_3^{\dagger} \right) a_{2,\mathrm{in}} \right] \\ &\quad + i \frac{\sqrt{6\kappa M}}{2} \left[- \left(c_3^{\dagger} + c_4^{\dagger} \right) a_{\mathrm{LA}}^{\dagger} + \left(c_3 + c_4 \right) a_{\mathrm{LA}} \right] \\ &\quad + i \sqrt{\frac{\kappa M}{2}} \left[\left(c_3 - c_4 \right) a_{\mathrm{BS}}^{\dagger} - \left(c_3^{\dagger} - c_4^{\dagger} \right) a_{\mathrm{BS}} \right]. \qquad (14) \end{aligned}$$

We assume that $a_{1,\mathrm{in}}$, $a_{2,\mathrm{in}}$, a_{LA}, and a_{BS} are all in vacuum states. The present model is a particular example of the cascaded quantum system which can be described by the input-output formalism of such a system (see, e.g., Ref. [6, 7]). In the language of quantum trajectories [7], the dynamics of the total system can be described by a non-Hermitian effective Hamiltonian

$$\begin{aligned} H_{\mathrm{eff}} &= \sum_{i=1}^{4} H_i - i\kappa \left[\frac{1}{2} \sum_{i=1}^{4} c_i^{\dagger} c_i + c_3^{\dagger} \left(c_1 + M c_2 \right) \right. \\ &\quad \left. + c_4^{\dagger} \left(c_2 + M c_1 \right) \right] \qquad (15) \end{aligned}$$

and two quantum-jump terms with Lindblad operators

$$L_1 = \sqrt{\kappa} \left(c_1 + c_3 \right), \quad L_2 = \sqrt{\kappa} \left(c_2 + c_4 \right). \qquad (16)$$

Here, we have omitted the dissipation terms proportional to the correction factor $M \ll 1$. Just like in Ref. [4], the following dark state condition should be satisfied to achieve coherent-state transmission

$$\left(c_1 + c_3 \right) |\psi\rangle = \left(c_2 + c_4 \right) |\psi\rangle = 0, \qquad (17)$$

where $|\psi\rangle$ is the state of the total system.

If the correction factor $M = 0$, the effective Hamiltonian can be expressed as

$$\begin{aligned} H_{\mathrm{eff}}^{0} &= \left[H_1 + H_3 - i\kappa \left(\frac{1}{2} c_1^{\dagger} c_1 + \frac{1}{2} c_3^{\dagger} c_3 + c_3^{\dagger} c_1 \right) \right] \\ &\quad + \left[H_2 + H_4 - i\kappa \left(\frac{1}{2} c_2^{\dagger} c_2 + \frac{1}{2} c_4^{\dagger} c_4 + c_4^{\dagger} c_2 \right) \right]. \\ &\qquad (18) \end{aligned}$$

The quantum channel composed of node 1, node 3, and the corresponding cavity modes represented by c_1, c_3 is separated from the quantum channel composed of node 2, node 4, and the cavity modes c_2, c_4. The state of the total system can then be assumed to be in the separable state

$$|\psi(t)\rangle = |\psi_{13}(t)\rangle \otimes |\psi_{24}(t)\rangle, \qquad (19)$$

where

$$\begin{aligned} |\psi_{13}\rangle &= \left\{ \sqrt{p_1} |g_1 g_3\rangle |0_1 0_3\rangle + \sqrt{1-p_1} \left[\alpha_1 |e_1 g_3\rangle |0_1 0_3\rangle \right. \right. \\ &\quad + \alpha_3 |g_1 e_3\rangle |0_1 0_3\rangle + \beta_1 |g_1 g_3\rangle |1_1 0_3\rangle \\ &\quad \left. \left. + \beta_3 |g_1 g_3\rangle |0_1 1_3\rangle \right] \right\}, \\ |\psi_{24}\rangle &= \left\{ \sqrt{p_2} |g_2 g_4\rangle |0_2 0_4\rangle + \sqrt{1-p_2} \left[\alpha_2 |e_2 g_4\rangle |0_2 0_4\rangle \right. \right. \\ &\quad + \alpha_4 |g_2 e_4\rangle |0_2 0_4\rangle + \beta_2 |g_2 g_4\rangle |1_2 0_4\rangle \\ &\quad \left. \left. + \beta_4 |g_2 g_4\rangle |0_2 1_4\rangle \right] \right\}. \end{aligned}$$

We can find the following evolution equations by comparing the coefficients of the Schrödinger equation

$$\begin{aligned} \dot{\alpha}_1 &= -g_1(t)\beta_1, \quad \dot{\alpha}_3 = -g_3(t)\beta_3, \\ \dot{\beta}_1 &= g_1(t)\alpha_1 + \kappa\beta_3, \quad \dot{\beta}_3 = g_3(t)\alpha_3 - \kappa\beta_1, \\ \dot{\alpha}_2 &= -g_1(t)\beta_2, \quad \dot{\alpha}_4 = -g_3(t)\beta_4, \\ \dot{\beta}_2 &= g_1(t)\alpha_2 + \kappa\beta_4, \quad \dot{\beta}_4 = g_3(t)\alpha_3 - \kappa\beta_2. \qquad (20) \end{aligned}$$

Here, we have set $g_2(t) = g_1(t)$ and $g_4(t) = g_3(t)$, which is reasonable because we have assumed that the four coupled atom-cavity systems are with the same system parameters. To solve Eq. (20), we can design the controls $g_i(t)$ $(i = 1, 2, 3, 4)$ by the Cirac-Zoller-Kimble-Mabuchi method (see Ref. [4])

$$\begin{aligned} g_3(t) &= g_1(-t), \quad \forall t \\ g_1(-t) &= \frac{-\sqrt{2}\kappa\beta_{13}(t) + g_1(t)\alpha_1(t)}{\alpha_3(t)}, \quad t > 0. (21) \end{aligned}$$

where α_1, β_{13} can be obtained by solving the equations

$$\begin{aligned} \dot{\alpha}_1 &= g_1(t)\beta_{13}/\sqrt{2}, \\ \dot{\beta}_{13} &= -\kappa\beta_{13} - \sqrt{2} g_1(t)\alpha_1, \qquad (22) \end{aligned}$$

with initial conditions

$$\begin{aligned} \alpha_1(0) &= \left[\frac{\kappa^2}{2\left(g_1^2(0) + \kappa^2 \right)} \right]^{1/2}, \\ \beta_{13}(0) &= \left[1 - 2\alpha_1^2(0) \right]^{1/2}; \qquad (23) \end{aligned}$$

and $\alpha_3(t)$ can be obtained by

$$\alpha_3(t) = \sqrt{1-\alpha_1^2(t)-\beta_{13}^2(t)}. \tag{24}$$

By such a design of the control pulses, we can realize a perfect state transmission from node 1 to node 3, and node 2 to node 4, such that

$$\begin{aligned}\alpha_1(-\infty) = \alpha_3(+\infty) = 1,\\ \alpha_2(-\infty) = \alpha_4(+\infty) = 1.\end{aligned} \tag{25}$$

For non-zero correction factor $M \ll 1$, the effective Hamiltonian can be expressed as

$$H_{\text{eff}} = H_{\text{eff}}^0 - i\kappa M\left(c_3^\dagger c_2 + c_4^\dagger c_1\right). \tag{26}$$

Since $M \ll 1$, we can assume that the system state still approximately resides in a separable state, but should include some other two-photon terms induced by the cross term $M\left(-i\kappa c_3^\dagger c_2 - i\kappa c_4^\dagger c_1\right)$ in H_{eff} (see Fig. 3).

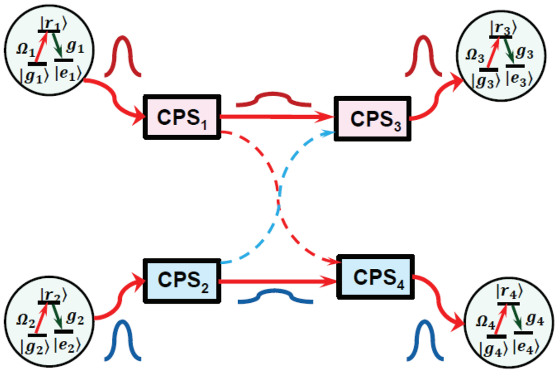

FIG. 3: (color online) Intersection of the two quantum channels when the correction factor $M \neq 0$.

The system state can then be expressed as

$$\begin{aligned}|\psi\rangle = &\Big\{\sqrt{p_1}|g_1g_3\rangle|0_10_3\rangle + \sqrt{1-p_1}\,[\alpha_1|e_1g_3\rangle|0_10_3\rangle\\ &+\alpha_3|g_1e_3\rangle|0_10_3\rangle + \beta_1|g_1g_3\rangle|1_10_3\rangle\\ &+\beta_3|g_1g_3\rangle|0_11_3\rangle]\Big\} \otimes \{\sqrt{p_2}|g_2g_4\rangle|0_20_4\rangle\\ &+\sqrt{1-p_2}\,[\alpha_2|e_2g_4\rangle|0_20_4\rangle + \alpha_4|g_2e_4\rangle|0_20_4\rangle\\ &+\beta_2|g_2g_4\rangle|1_20_4\rangle + \beta_4|g_2g_4\rangle|0_21_4\rangle]\}\\ &+[\beta_5|g_1g_3\rangle|0_12_3\rangle|g_2g_4\rangle|0_20_4\rangle\\ &+\alpha_5|g_1e_3\rangle|0_11_3\rangle|g_2g_4\rangle|0_20_4\rangle]\\ &+[\beta_6|g_1g_3\rangle|0_10_3\rangle|g_2g_4\rangle|0_22_4\rangle\\ &+\alpha_6|g_1g_3\rangle|0_10_3\rangle|g_2e_4\rangle|0_21_4\rangle].\end{aligned} \tag{27}$$

By comparing the coefficients of the Schrödinger equation and letting $g_1(t) = g_2(t)$ and $g_3(t) = g_4(t)$, we can find the following dynamical equations

$$\begin{aligned}\dot{\alpha}_1 &= -g_1(t)\,\beta_1, & \dot{\tilde{\alpha}}_3 &= -g_3(t)\,\tilde{\beta}_3,\\ \dot{\beta}_1 &= g_1(t)\,\alpha_1 + \kappa\tilde{\beta}_3, & \dot{\tilde{\beta}}_3 &= g_3(t)\,\tilde{\alpha}_3 - \kappa\beta_1,\\ \dot{\alpha}_2 &= -g_1(t)\,\beta_2, & \dot{\tilde{\alpha}}_4 &= -g_3(t)\,\tilde{\beta}_4,\\ \dot{\beta}_2 &= g_1(t)\,\alpha_2 + \kappa\tilde{\beta}_4, & \dot{\tilde{\beta}}_4 &= g_3(t)\,\tilde{\alpha}_4 - \kappa\beta_2,\end{aligned} \tag{28}$$

where

$$\begin{aligned}\tilde{\alpha}_3 &= \alpha_3 + M\left[\sqrt{p_1(1-p_2)}/\sqrt{p_2(1-p_1)}\right]\alpha_4,\\ \tilde{\alpha}_4 &= \alpha_4 + M\left[\sqrt{p_2(1-p_1)}/\sqrt{p_1(1-p_2)}\right]\alpha_3,\\ \tilde{\beta}_3 &= \beta_3 + M\left[\sqrt{p_1(1-p_2)}/\sqrt{p_2(1-p_1)}\right]\beta_4,\\ \tilde{\beta}_4 &= \beta_4 + M\left[\sqrt{p_2(1-p_1)}/\sqrt{p_1(1-p_2)}\right]\beta_3.\end{aligned} \tag{29}$$

Comparing Eqs. (20) and (28), we can see that the dynamical equations for α_i, β_i, $i = 1,2,3,4$ and the equations for α_1, α_2, $\tilde{\alpha}_3$, $\tilde{\alpha}_4$, β_1, β_2, $\tilde{\beta}_3$, $\tilde{\beta}_4$ are the same. We can design the controls $g_i(t)$ $(i = 1,2,3,4)$ by simply replacing α_3, α_4, β_3, β_4, by $\tilde{\alpha}_3$, $\tilde{\alpha}_4$, $\tilde{\beta}_3$, and $\tilde{\beta}_4$ in Eqs. (21), (22), and (23). Then we have

$$\tilde{\alpha}_3(+\infty) = \tilde{\alpha}_4(+\infty) = 1, \tag{30}$$

which means that

$$\begin{aligned}\alpha_3(+\infty) &= 1 - M\left[\frac{\sqrt{p_1(1-p_2)}}{\sqrt{p_2(1-p_1)}}\right] + O(M^2),\\ \alpha_4(+\infty) &= 1 - M\left[\frac{\sqrt{p_2(1-p_1)}}{\sqrt{p_1(1-p_2)}}\right] + O(M^2),\end{aligned} \tag{31}$$

where $O(M^2)$ represents higher-order terms of M under the condition that $M \ll 1$. It can be further checked that $\beta_5(+\infty) = \beta_6(+\infty) = 0$. To solve $\alpha_5(+\infty)$, $\alpha_6(+\infty)$, we can see that the reduced state of the system composed of atom 3 and atom 4 can be written as

$$\begin{aligned}\rho_{34}(t) = &\Big[\left(\sqrt{p_1}|g_3\rangle + \sqrt{1-p_1}\alpha_3(+\infty)|e_3\rangle\right)\\ &\left(\sqrt{p_2}|g_4\rangle + \sqrt{1-p_2}\alpha_4(+\infty)|e_4\rangle\right)\Big]\\ &\Big[\left(\sqrt{p_1}\langle g_3| + \sqrt{1-p_1}\alpha_3(+\infty)\langle e_3|\right)\\ &\left(\sqrt{p_2}\langle g_4| + \sqrt{1-p_2}\alpha_4(+\infty)\langle e_4|\right)\Big]\\ &+\alpha_5^2(+\infty)|e_3g_4\rangle\langle e_3g_4|\\ &+\alpha_6^2(+\infty)|g_3e_4\rangle\langle g_3e_4|.\end{aligned} \tag{32}$$

From $\mathrm{tr}[\rho_{34}(t)] = 1$, we have

$$\begin{aligned}&\alpha_5^2(+\infty) + \alpha_6^2(+\infty)\\ &= 1 - \left[p_1 + (1-p_1)\,\alpha_3^2(+\infty)\right]\left[p_2 + (1-p_2)\,\alpha_4^2(+\infty)\right]\\ &= 2M\sqrt{p_1p_2(1-p_1)(1-p_2)}\left(\frac{1}{p_1} + \frac{1}{p_2}\right) + O(M^2).\end{aligned}$$

Further, from the symmetry of the system Hamiltonian (26), we have $\alpha_5(+\infty) = \alpha_6(+\infty)$, which means that

$$\begin{aligned} & \alpha_5^2(+\infty) = \alpha_6^2(+\infty) \\ = \ & M\sqrt{p_1 p_2 (1-p_1)(1-p_2)}\left(\frac{1}{p_1}+\frac{1}{p_2}\right) + O(M^2). \end{aligned}$$

From Eq. (32), it can be shown that the reduced states of atom 3 and atom 4 in the long-time limit can be expressed respectively as

$$\begin{aligned} \rho_3(+\infty) &= \left[p_2 + (1-p_2)\alpha_4^2(+\infty)\right] \\ & \left[\sqrt{p_1}|g_3\rangle + \sqrt{1-p_1}\alpha_3(+\infty)|e_3\rangle\right] \\ & \left[\sqrt{p_1}\langle g_3| + \sqrt{1-p_1}\alpha_3(+\infty)\langle e_3|\right] \\ & +\alpha_5^2(+\infty)|e_3\rangle\langle e_3| + \alpha_6^2(+\infty)|g_3\rangle\langle g_3|, \\ \rho_4(+\infty) &= \left[p_1 + (1-p_1)\alpha_3^2(+\infty)\right] \\ & \left[\sqrt{p_2}|g_4\rangle + \sqrt{1-p_2}\alpha_4(+\infty)|e_4\rangle\right] \\ & \left[\sqrt{p_2}\langle g_4| + \sqrt{1-p_2}\alpha_4(+\infty)\langle e_4|\right] \\ & +\alpha_5^2(+\infty)|e_4\rangle\langle e_4| + \alpha_6^2(+\infty)|g_4\rangle\langle g_4|. \end{aligned}$$

Thus, we can calculate the final fidelities of the state transmission through the two channels

$$\begin{aligned} F_1 &= \left(\sqrt{p_1}\langle g_3| + \sqrt{1-p_1}\langle e_3|\right)\rho_3(+\infty) \\ & \left(\sqrt{p_1}|g_3\rangle + \sqrt{1-p_1}|e_3\rangle\right) \\ &= \left[p_2 + (1-p_2)\alpha_4^2(+\infty)\right] \\ & \left[p_1 + (1-p_1)\alpha_3(+\infty)\right]^2 \\ & +M\sqrt{p_1 p_2(1-p_1)(1-p_2)}\left(\frac{1}{p_1}+\frac{1}{p_2}\right) \\ &= 1 - M\sqrt{p_1 p_2(1-p_1)(1-p_2)}\left(\frac{1}{p_1}+\frac{1}{p_2}\right), \\ & +O(M^2) \\ F_2 &= \left(\sqrt{p_2}\langle g_4| + \sqrt{1-p_2}\langle e_4|\right)\rho_4(+\infty) \\ & \left(\sqrt{p_2}|g_4\rangle + \sqrt{1-p_2}|e_4\rangle\right) \\ &= \left[p_1 + (1-p_1)\alpha_3^2(+\infty)\right] \\ & \left[p_2 + (1-p_2)\alpha_4(+\infty)\right]^2 \\ & +M\sqrt{p_1 p_2(1-p_1)(1-p_2)}\left(\frac{1}{p_1}+\frac{1}{p_2}\right) \\ &= 1 - M\sqrt{p_1 p_2(1-p_1)(1-p_2)}\left(\frac{1}{p_1}+\frac{1}{p_2}\right) \\ & +O(M^2). \end{aligned} \tag{33}$$

If the transmitted quantum states are

$$|\phi_1\rangle = \sqrt{p_0}|g_1\rangle + \sqrt{1-p_0}|e_1\rangle$$

and

$$|\phi_2\rangle = \sqrt{1-p_0}|g_2\rangle + \sqrt{p_0}|e_2\rangle,$$

i.e., $p_1 = p_0$, $p_2 = 1-p_0$, it can be calculated from Eq. (33) that

$$F_1 = F_2 = 1 - M + O(M^2). \tag{34}$$

CHAOTIC SYNCHRONIZATION OF DUFFING OSCILLATORS

We will analyze the chaotic synchronization of the two driven Duffing oscillators shown in Fig. 4 induced by the harmonic interaction potential $V(x_1, x_3) = k_I (x_1 - x_3)^2/2$, and give an estimate of the bound of the interaction strength k_I.

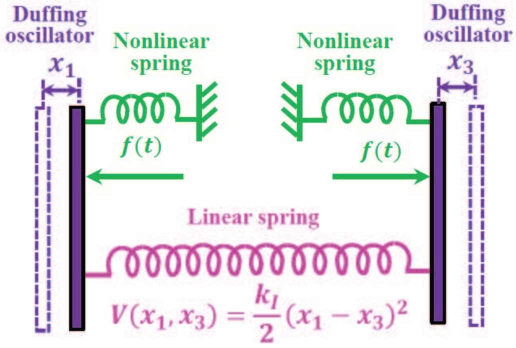

FIG. 4: (color online) Schematic diagram of the chaotic synchronization realized by the moving mirrors.

The dynamics of the two coupled Duffing oscillators is described by

$$\begin{aligned} \dot{x}_1 &= \omega_0 p_1 - \frac{\gamma}{2}x_1, \\ \dot{p}_1 &= -\omega_0 x_1 + 4\mu x_1^3 + f(t) - k_I(x_1 - x_3) - \frac{\gamma}{2}p_1, \\ \dot{x}_3 &= \omega_0 p_3 - \frac{\gamma}{2}x_3, \\ \dot{p}_3 &= -\omega_0 x_3 + 4\mu x_3^3 + f(t) - k_I(x_3 - x_1) - \frac{\gamma}{2}p_3. \end{aligned} \tag{35}$$

From these, we can obtain the equations of the differences of the positions and momenta of the two oscillators, $e_x = x_1 - x_3$ and $e_p = p_1 - p_3$, as

$$\begin{aligned} \dot{e}_x &= \omega_0 e_p - \frac{\gamma}{2}e_x, \\ \dot{e}_p &= (-\omega_0 + 4\mu X - 2k_I)e_x - \frac{\gamma}{2}e_p, \end{aligned}$$

where

$$X = x_1^2 + x_1 x_3 + x_3^2.$$

Since the eigen-equation of the linear matrix of the above equation is

$$\lambda^2 + \gamma\lambda + \frac{\gamma^2}{4} + \omega_0^2 - 4\mu X\omega_0 + k_I\omega_0 = 0,$$

it can be verified that the chaotic synchronization, i.e., e_x, $e_p \to 0$, occurs when

$$k_I \ > \ 4\mu B - \frac{\gamma^2}{4\omega_0} - \omega_0, \tag{36}$$

where B is the upper bound of $|X|$, i.e., $|X| \leq B$. Equation (36) shows that the two chaotic oscillators synchronize only when the strength k_I of the harmonic interaction potential $V(x_1, x_3)$ is *strong* enough.

To estimate the lower bound of k_I to achieve chaotic synchronization, let us give an estimation of B. Since

$$|X| \leq |x_1|^2 + |x_1||x_3| + |x_3|^2,$$

we just need to estimate the upper bounds of $|x_1|$ and $|x_3|$. Assume that the two Duffing oscillators have synchronized, then we have $(x_1 - x_3) \to 0$. Thus we only need to estimate the bound of x_1, and omit the cross term $-k_I(x_1 - x_3)$ in Eq. (35) to obtain the equations of x_1 and p_1 as

$$\begin{aligned} \dot{x}_1 &= \omega_0 p_1 - \frac{\gamma}{2} x_1, \\ \dot{p}_1 &= -\omega_0 x_1 + 4\mu x_1^4 + f(t) - \frac{\gamma}{2} p_1. \end{aligned} \tag{37}$$

To estimate the bound of x_1, we introduce the harmonic balance approach, by which we can omit the high-frequency components and assume that

$$x_1 = A \cos(\omega_d t + \phi). \tag{38}$$

Substituting Eq. (38) into Eq. (37), we can obtain the following equations by comparing the coefficients of the terms $\cos(\omega_d t + \phi)$ and $\sin(\omega_d t + \phi)$

$$\left(-\frac{\omega_d^2}{\omega_0} + \omega_0 + \frac{\gamma^2}{4\omega_0}\right) A - 3\mu A^3 = f_d \cos\phi,$$
$$-\frac{\gamma\omega_d}{\omega_0} A = f_d \sin\phi.$$

Eliminating the unknown parameter ϕ, we can obtain the algebraic equation to solve the bound A of $|x_1|$

$$A^2 \left[\left(1+\gamma^2\right) \frac{\omega_d^2}{\omega_0^2} - \frac{\gamma^2}{\omega_0} - \omega_0 + 3\mu A^2\right]^2 = f_d^2. \tag{39}$$

Then, we can verify with simple calculations that the two Duffing oscillators synchronize only if the coupling strength k_I between them is large enough such that

$$k_I > 12\mu A^2 - \frac{\gamma^2}{4\omega_0} - 2\omega_0, \tag{40}$$

where the parameter A is solved numerically from Eq. (39).

We now show some numerical results, using the system parameters

$$(\omega_d, g_{\text{f}-\text{o}}, \mu, \gamma, k_I) = (5\omega_0, 0.03\omega_0, 0.25\omega_0, 0.05\omega_0, 0.1\omega_0).$$

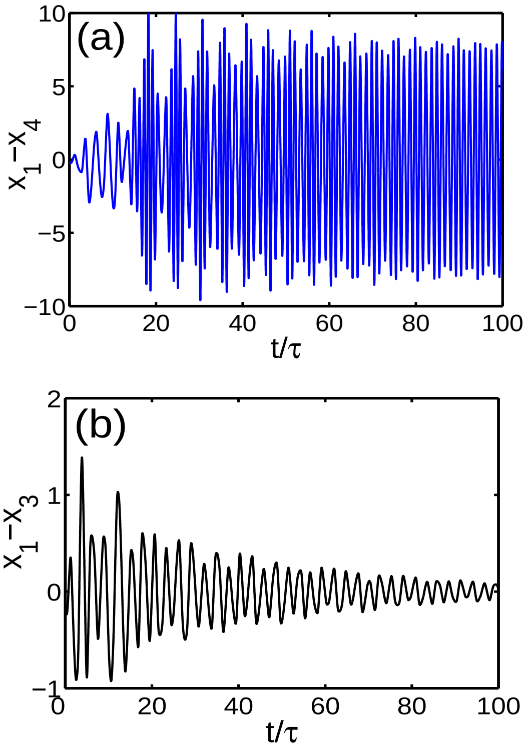

FIG. 5: (color online) Chaotic synchronization: (a) the blue curve shows the difference $(x_1 - x_4)$ (the unsynchronized case) and (b) the black curve shows the difference $(x_1 - x_3)$, with $k_I = 0.1\omega_0$ (the synchronized case).

In Fig. 5, we show the chaotic synchronization induced by the harmonic interaction potential $V(x_1, x_3)$. Here, we set $f_d/\omega_0 = 36$, where the dynamics of CPS$_{i=1,2,3,4}$ (the Duffing oscillators) are all in the chaotic regime. In Fig. 5(a), the normalized position x_1 of CPS$_1$ and x_4 of CPS$_4$ are unsynchronized in the long-time limit due to the lack of the harmonic interaction. In this case, the small difference in the initial condition is amplified in the long-time limit due to the sensitivity to the initial condition of the chaotic motion. In Fig. 5(b), the difference between the position x_1 of CPS$_1$ and x_3 of CPS$_3$ tends to zero, which means that x_1 and x_3 are synchronized under the harmonic interaction potential $V(x_1, x_3)$. From the parameters chosen in our simulation, it can be estimated from Eq. (40) that $k_I > 0.08\omega_0$. Thus, the two Duffing oscillators synchronize with $k_I = 0.1\omega_0$ in our simulation results shown in Fig. 5(b).

---

[*] Electronic address: jing-zhang@mail.tsinghua.edu.cn

[1] L. Zhou, S. Yang, Y. X. Liu, C. P. Sun, and F. Nori, Phys. Rev. A **80**, 062109 (2009); S. Ashhab, J. R. Johansson, A. M. Zagoskin, and F. Nori, Phys. Rev. A **75**, 063414 (2007).
[2] J. Zhang, Y. X. Liu, W. M. Zhang, L. A. Wu, R. B. Wu,

and T. J. Tarn, Phys. Rev. B **84**, 214304 (2011).

[3] J. Bergli, Y. M. Galperin, and B. L. Altshuler, New J. Phys. **2**, 025002 (2009).

[4] J. I. Cirac, P. Zoller, H. J. Kimble, and H. Mabuchi, Phys. Rev. Lett. **78**, 3221 (1997); S. J. Van Enk, J. I. Cirac, P. Zoller, H. J. Kimble, and H. Mabuchi, J. Mod. Opt. **44**, 10, 1727.

[5] D.F.V. James and J. Jerke, Can. J. Phys. **85**, 625 (2007).

[6] C. W. Gardiner, Phys. Rev. Lett. **70**, 2269 (1993).

[7] H. J. Carmichael, Phys. Rev. Lett. **70**, 2273 (1993).